ANTICANCER RESEARCH *41*: 4807-4820 (2021)
doi:10.21873/anticanres.15296

Synergistic Antitumor Effect of Taxanes and CDK4/6 Inhibitor in Lung Cancer Cells and Mice Harboring KRAS Mutations

KYOUNG-HWA SON[1,2], MIN-YOUNG KIM[1,2], JUNG-YOUNG SHIN[1], JEONG-OH KIM[1] and JIN-HYOUNG KANG[1,2,3]

[1]*Laboratory of Medical Oncology, Cancer Research Institute, College of Medicine, The Catholic University of Korea, Seoul, Republic of Korea;*
[2]*Department of Biomedicine & Health Sciences, Seoul, Republic of Korea;*
[3]*Department of Medical Oncology, Seoul St. Mary's Hospital, The Catholic University of Korea, Seoul, Republic of Korea*

Abstract. *Background/Aim: LY2835219 (LY), a novel CDK4/6 inhibitor, prevents cell proliferation through G1 arrest. Docetaxel (DTX) and paclitaxel (PTX) are cytotoxic drugs targeting tubulin-mediated apoptotic cell death via G2/M arrest. We evaluated the antitumor effects of DTX/PTX and LY individually and in combination in lung adenocarcinoma cells with or without KRAS mutations and xenograft mice harboring KRAS mutations. Materials and Methods: We investigated in vitro/in vivo changes in signaling molecules and analyzed cell proliferation, cycle, and apoptosis via flow cytometry and western blotting. Results: LY cytotoxicity was dose-dependent and varied with KRAS mutation status. DTX→LY showed synergistic cytotoxicity regardless of KRAS mutation. Furthermore, the synergistic effect of PTX→LY was significantly greater than that of PTX+LY. DTX→LY remarkably reduced the number of G0/G1 cells and increased the number of G2/M arrested cells, resulting in an increase in apoptosis and subG1 cells. Conclusion: DTX→LY has synergistic antitumor effect in lung cancer cells and xenograft mice regardless of KRAS mutation.*

Lung cancer is the leading of cancer cause death worldwide, and adenocarcinoma is the most common histological subtype (1). In lung adenocarcinoma, *KRAS* is the most frequently mutated oncogene, with activating, gain-of-function mutations in codon 12, 13, or 61 (2). This oncogene constitutively activates the RAS/RAF/ERK signaling pathway, leading to regulation of tumor cell proliferation and survival (3-5).

Cyclin-dependent kinases (CDK), the enzyme family regulating the cell cycle, are frequently found to be over-expressed in various cancers. CDK4/6 also plays a major role in stimulating the G1/S phase transition in cell cycle, resulting in cell growth, and promoting tumorigenesis (2, 6, 7). Genetic alterations in CDK4/6 result in poor prognosis in non-small cell lung cancer (NSCLC) harboring *KRAS* mutations. Accordingly, CDK4/6 may be a potential drug target in lung adenocarcinomas harboring *KRAS* mutations (8, 9).

LY2835219 (LY), a novel CDK4/6 inhibitor, effectively prevents Retinoblastoma protein (RB) phosphorylation and E2F activation, thereby arresting the cell cycle in the G1 phase and suppressing cell proliferation and cell division (10). Taxanes, such as docetaxel (DTX) and paclitaxel (PTX), are cytotoxic anticancer drugs that inhibit the mitotic phase of the cell cycle by blocking microtubules, thereby resulting in G2/M arrest and apoptosis (11, 12).

Previous studies demonstrated that LY combined with vemurafenib, a BRAF-selective inhibitor, is an effective treatment for overcoming MAPK-mediated resistance to BRAF inhibitors in a melanoma mouse model (13). Chen *et al*. discovered that the sequential treatment with DTX and gefitinib induced synergistic antiproliferative activity in EGFR-tyrosine kinase inhibitors (TKIs) resistant A549^{G12S} cells (14). These results indicate that the combination therapy can enhance the antitumor effect, leading to prolonged progression-free survival. The synergistic antitumor activity of drug combinations helps in mitigating serious drug adverse reactions caused by administration of high doses of a drug for inhibiting tumor cell proliferation and growth (15-17).

In our previous study on sequential treatment of *KRAS*- and *BRAF*-mutant NSCLC cells with PTX and a RAF

Correspondence to: Jin-Hyoung Kang, MD, Ph.D., Department of Medical Oncology, Seoul St. Mary's Hospital, The Catholic University of Korea, 222, Banpo-daero, Seocho-gu, Seoul 06591, Republic of Korea. Tel: +82 222586043, Fax: +82 25338450, e-mail: oncologykang@naver.com

Key Words: Docetaxel, paclitaxel, CDK4/6 inhibitor, synergism, *KRAS* mutation, lung cancer.

kinase inhibitor, a synergistic interaction between the drugs was observed (18). We demonstrated that combination therapy with a CDK4/6 inhibitor (CINK4) and PTX had enhanced antitumor effect on lung adenocarcinomas harboring *KRAS* mutation.

The aim of this study was to evaluate the effect of the treatment with DTX+LY on cell proliferation and cycle, and apoptosis in lung adenocarcinoma cells and xenograft mice with or without *KRAS* mutations. We also investigated the changes in signaling molecules involved in the anti-proliferative activity of the combination therapy.

Materials and Methods

Cell lines. The human lung carcinoma cell lines A549^{G12S} (*KRAS*^{G12S}), H727^{G12V} (*KRAS*^{G12V}), and H1666^{WT} (*KRAS*^{WT}) were obtained from the Korean Cell Line Bank (KCLB; Seoul, Korea), and Calu-3^{WT} (*KRAS*^{WT}) was obtained from the American Type Culture Collection (ATCC; Manassas, VA, USA). A549^{G12S} cells were propagated in RPMI 1640 medium (WelGENE, Seoul, Korea) supplemented with 10% fetal bovine serum (FBS; Gibco BRL, Waltham, MA, USA). H727^{G12V}, Calu-3^{WT}, and H1666^{WT} cells were maintained in Dulbecco's Modified Eagle Medium (DMAEM) (WelGENE, Seoul, Republic of Korea). The cells were incubated at 37˚C in humidified atmosphere containing 5% CO_2.

Animals. Male BALB/c nu/nu mice (20 g weight; 4 weeks old; Orient Animal Laboratory, Seoul, Korea) were used in this study. The total number of mice used was thirty, and they were maintained under standard conditions and received food and water ad libitum (Breeding environment Temperature: 20-26˚C, Humidity: 50±10%, 12-h light-dark cycle). All procedures of animal research were performed in accordance with the Laboratory Animals Welfare Act, the Guide for the Care and Use of Laboratory Animals, and the Guidelines and Policies for Rodent experiment provided by the IACUC (Institutional Animal Care and Use Committee) of the School of Medicine, The Catholic University of Korea (Approval number: CUMC-2014-0187-02). IACUC and Department of Laboratory Animal (DOLA) of the Catholic University of Korea, Songeui Campus were accredited the Korea Excellence Animal Laboratory Facility from Korea Food and Drug Administration in 2017.

Experimental drugs. Docetaxel (DTX) was provided by KORAM Biotech Corporation (Seoul, Republic of Korea) and LY2835219 (LY; CDK4/6 inhibitor) was donated by Lilly (Indianapolis, IN, USA). For *in vitro* experiments, LY and DTX were dissolved in 100% DMSO (Sigma, St. Louis, MO, USA) and diluted with culture medium to the desired concentration with a final DMSO concentration of 0.1%. For *in vivo* experiments, LY was formulated in 1% hydroxyethyl cellulose+0.1% antifoam in 25 mM phosphate buffer (PB) pH 2. Paclitaxel (PTX) was dissolved in Cremophor EL/95% ethanol (50:50) at four times the highest dose for each.

Drug combination effect. We selected the drug concentrations and treatment times based on the cytotoxicity of a single drug (between 0.0003 nM and 300 nM in A549^{G12S} and Calu-3^{WT} cells, between 0.0003 nM and 100 nM in H727^{G12V} cells). The concentrations of LY administered with DTX were 0.03 μM and 0.3 μM.

The three lung cancer cell lines were simultaneously (DTX+LY) and sequentially treated with DTX for 24 h followed by LY treatment for 48 h (DTX→LY). The control wells comprised cells incubated with culture medium. Interactions between DTX and LY were calculated using the combination index (CI=D1/Df1+D2/Df2+D1D2/Df1Df2). The calculated CI was divided into 3 categories (CI<1, CI=1, or CI>1, indicating synergistic, additive, and antagonistic effects, respectively).

Cell proliferation assay. Cells were seeded at 3×10^3 or 5×10^3 per well in 96-well sterile plastic dishes (Thermo, Waltham, MA, USA), allowed to attach for 24 h, and treated with single-drug dilutions. The cells were treated with a series of final concentrations ranging from 0.00003 μM to 100 μM for LY and from 0.00003 nM to 300 nM for DTX for 72 h. The inhibition of cell growth was determined using Cell Counting Kit-8 assay (Dojindo, Japan) according to the manufacture's protocol. The absorbance was measured at 450 nm using an enzyme-linked immunosorbent assay (ELISA) reader (PowerWave XS, BIO-TEK, VT, USA).

Cell cycle analysis. Cells were seeded at 1×10^5 and incubated for 72 h. After the treatments were completed, cells were trypsinized, washed twice with PBS, and harvested *via* centrifugation. Then, cells were fixed with ice-cold 70% ethanol for at least 12 h. After removing the ethanol and washing twice with cold PBS, the cells were resuspended in 1 m of PBS and stained with propidium iodide (PI) solution (0.05 mg/ml PI, 10 mg/ml RNase A) for 20 min at 37˚C in the dark room. The fluorescence of PI-stained cells was measured *via* flow cytometry (BD FACS Canto II, Becton Dickinson, Franklin Lakes, NJ, USA); at least 1×10^4 cells were counted, and the DNA content was analyzed using CellQuest software (Becton Dickinson). All experiments were performed in triplicate.

Apoptosis assay. Cells were seeded at a density of 1×10^5 and incubated for 72 h before treatment. Following this, adherent and non-adherent cells were harvested and apoptotic cells were detected using an FITC Annexin V Apoptosis Detection Kit I (Cat. #556547, BD PharMingen, Franklin Lakes, NJ, USA) according to the manufacturer's protocol. In brief, cells were washed with cold PBS, resuspended in 1× binding buffer (0.1 M HEPES/NaOH, pH 7.4, 1.4 M NaCl, and 25 mM $CaCl_2$), stained with annexin V-FITC and PI, incubated for 15 min at room temperature in a dark room, and analyzed *via* flow cytometry (BD FACS Canto II). All experiments were performed in triplicate.

Western blot analysis. Cells were seeded at a density of 1×10^5 cells in 100-mm plastic dishes and incubated for 72 h before the addition of the drug. After drug treatment, cells were harvested with trypsin/EDTA, washed twice with PBS, and lysed with RIPA cell lysis buffer (Gibco BRL) containing a protease inhibitor cocktail (Amresco, Solon, OH, USA). Proteins from each cell treatment were resolved on 10% SDS polyacrylamide gels (SDS-PAGE) and transferred onto PVDF membranes. Primary antibodies against CDK4 (Cat. #12790s; 1:1,000), cyclin B1 (Cat. #12231p; 1:1,000), p21 (Cat. #2947p; 1:1,000), cleaved-PARP (Cat. #9541s; 1:1,000), cleaved-caspase-3 (Cat. #9661s; 1:1,000), total PARP (Cat. #9542s; 1:1,000), total caspase-3 (Cat. #9662s; 1:1,000), p-ERK (Cat. #9101s; 1:1,000), total ERK (Cat. #9102s; 1:1,000), MEK1/2 (Cat. #9122; 1:1,000) were purchased from Cell Signaling Technology

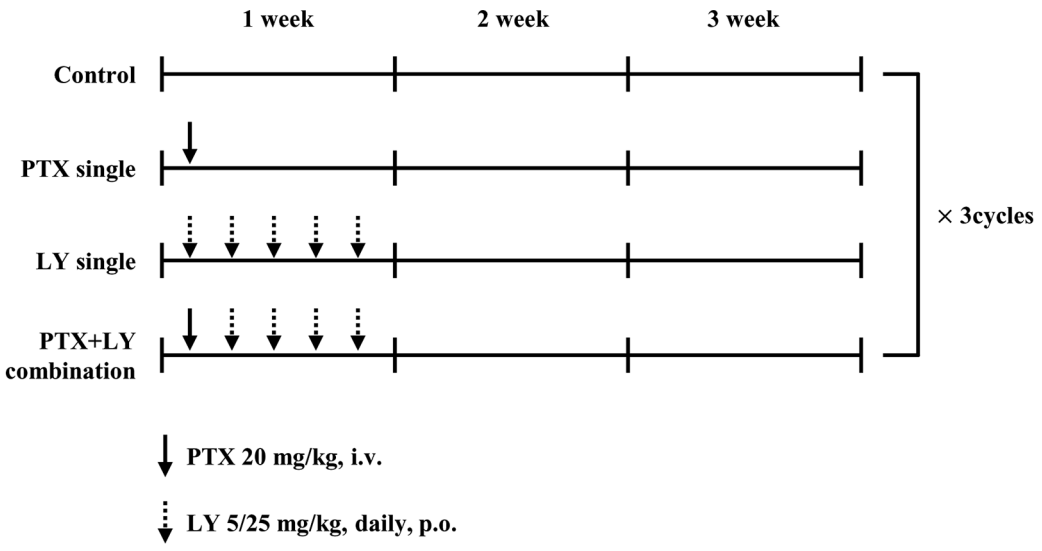

Figure 1. *The schedule for PTX and LY alone and/or combination treatment. The dose of LY (5 mg/kg and 25 mg/kg, once daily, oral administration; p. o.) and PTX (20 mg/kg, once per week, intravenous injection; i. v.). BALB/c nu/nu mice were divided into six groups (control, PTX20 mg/kg, LY5 mg/kg, LY25 mg/kg, PTX+LY5 mg/kg and PTX+LY25 mg/kg; n=5 per group).*

(Danvers, MA, USA) overnight at 4˚CCDK2 (cat. no. 51-9001919; 1:1,000) was obtained from BD PharMingen and KRAS (Cat. #sc-30; 1:1,000) from Santa Cruz Biotechnology (Dallas, Texas, USA). β-actin (Cat. #G043; 1:1,000), and GAPDH (Cat. #G043; 1:1,000) were purchased from Applied Biological Materials Inc. (Richmond, BC, Canada). Following incubation at 4^{O}C overnight with the primary antibodies, the membrane was washed and incubated with HRP-conjugated secondary antibodies (Cat. #GTX213110-01; 1:2,000; Genetex, Alton Pkwy Irvine, CA, USA), and Cat. #7076S; Cell Signaling Technology) for 1 h.

Tumor xenograft model. Tumor xenograft models were established by subcutaneously injecting A549^{G12S} or H727^{G12V} tumor cells into 4-week-old female BALB/c nu/nu mice. Mice were randomized into control and treatment groups. When the tumor volume reached 400-500 mm^3, the mice were treated with drugs (Figure 1). The dose of LY (5 mg/kg and 25 mg/kg, once daily, oral administration; *p.o.*) and PTX (20 mg/kg, once per week, intravenous injection; *i.v.*) have been previously reported (2). Tumor dimensions and body weight were measured twice a week. Treatment schedules resulting in greater than 20% lethality and/or 20% net body weight loss were considered highly toxic. All mice were inhaled with 5% isoflurane using Anesthesia Machine (Harvard Apparatus Fluovac Anesthetizing System, MA, USA) and maintained at 2.5% after respiration was stabilized. At the end of the experiment, mice were euthanized with CO_2 gas of 30-70% chamber volume/min for at least 5 min and then cardiac arrest was confirmed. Tumor tissues were immediately removed for subsequent analysis.

Statistical analysis. All data obtained from at least three independent experiments are presented as the mean±the standard deviation or median±interquartile range. Statistical analysis was performed using PASW Statistics version 18.0 (SPSS, Inc., Chicago, IL, USA). Significance was tested using one-way ANOVA and Tukey's *post hoc* test for multiple comparisons. A *p*-value of <0.05 was considered to indicate a statistically significant difference. All experiments were analyzed using Microsoft Excel 2010 for Windows 7 (Microsoft, Seoul, Republic of Korea) and PASW Statistics version 18.0 (SPSS Inc.).

Results

Anti-proliferative effect of DTX and LY. To evaluate the anti-proliferative effect of DTX and LY in lung cancer cells with or without *KRAS* mutations, we measured the cancer cell viability after 72 h of treatment with DTX (0.00003, 0.1, 1, 10, 100, and 300 nM) or LY (0.00003, 0.0003, 0.3, 3, 30, and 100 μM) using the CCK-8 assay.

The IC50 of DTX was 4.8±0.2 nM and 11.3±0.2 nM in A549^{G12S} and H727^{G12V} cells, respectively, and 6.0±2.8 nM and 18.5±1.3 nM in Calu-3^{WT} and H1666^{WT} cells, respectively (Figure 2A). The IC50 of PTX was 3.8±0.8 nM and 6.4±5.0 nM in A549^{G12S} and H727^{G12V} cells, respectively, and 16.9±2.9 nM and 18.0±1.2 nM in Calu-3^{WT} and H1666^{WT} cells, respectively. A549^{G12S} cells were the most sensitive to PTX treatment and cytotoxicity was lower in cancer cells with wild-type *KRAS* (Figure 2B). The IC50 of LY was 1.0±0.2 μM and 2.6±0.3 μM in A549^{G12S} and H727^{G12V} cells and 1.3±.1 μM and 32.3 ±0.01 μM in Calu-3^{WT} and H1666^{WT} cells, respectively (Figure 2C). Among the four lung cancer cells, A549^{G12S} cells were the most sensitive to the two drugs. The cell growth inhibitory effect of these drugs was lower in cancer cells with wild-type *KRAS* compared with cancer cells with *KRAS* mutant.

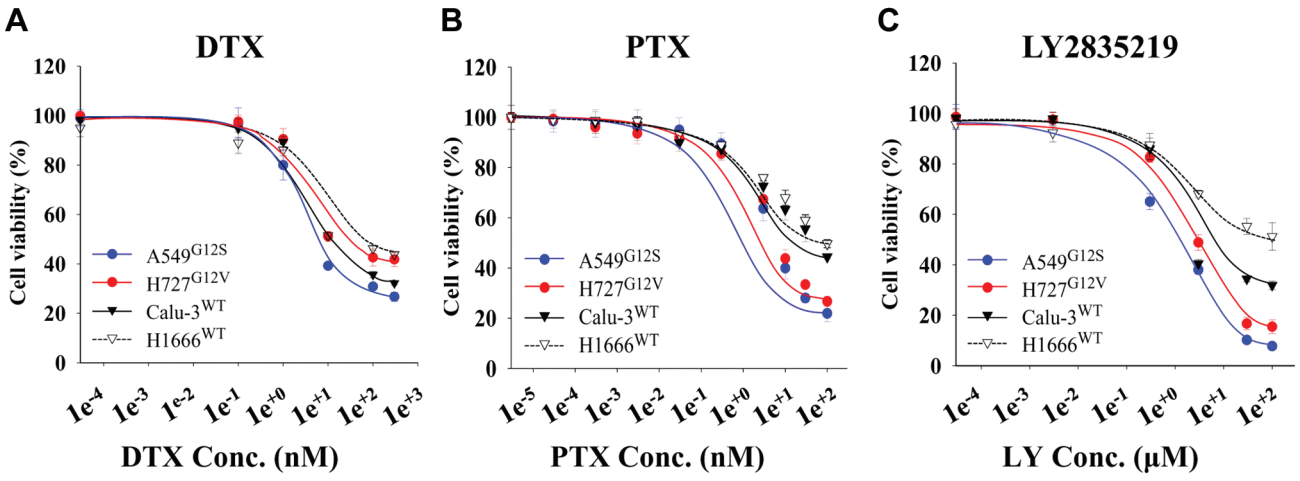

Figure 2. *The anti-proliferative effects of DTX and LY in lung cancer cell lines. (A) DTX and (B) LY (72 h) inhibited cell proliferation in a dose-dependent manner. A549^{G12S}, H727^{G12V}, Calu-3^{WT}, H1666^{WT} cells were measured using the CCK-8 assay and presented as a percentage of the total cell population. Each experiment was performed in triplicate. Data are presented as the mean±SD.*

Even the highest concentration of DTX and LY inhibited the percent of viable lung cancer cells with wild-type *KRAS* only by 30-40%. In contrast, LY reduced the percentage of viable lung cancer cells with *KRAS* mutations by 10-20%.

Anti-proliferative effect of simultaneous or sequential DTX+LY treatment. We evaluated the anti-proliferative effect of simultaneous and sequential combination therapy with DTX or PTX and LY and compared it with DTX or PTX treatment alone. On the basis of the previous results of individual drug treatment, A549^{G12S}, H727^{G12V}, and Calu-3^{WT} cells were treated with various concentrations of DTX and 0.03 and 0.3 μM LY. There were two treatment schedules: simultaneous (DTX+LY) and sequential (DTX→LY). In A549^{G12S} cells, the cytotoxicity with DTX (0.1 nM) →LY (0.003 μM) treatment was not very different from DTX treatment alone (percent of viable cells: 97.7±0.7%), but the cytotoxicity was significantly enhanced with the increase in LY concentration from 0.03 to 0.3 μM (percent of viable cells: 52.7±0.7% and 35.7±0.8%, respectively, $p<0.001$). At 100 nM DTX, there was no enhancement in cytotoxicity, even with increased LY concentrations. In H727^{G12V} cells, the cytotoxicity with DTX→LY treatment was significantly higher than that with DTX treatment alone (percent of viable cells: 58.9±0.5% and 48.8±0.6% *vs.* 98.3±0.8%, $p<0.001$); the cytotoxicity gradually increased with the escalation of LY concentration. In Calu-3^{WT} cells, the cytotoxicity with DTX→LY treatment was dependent on LY concentration and was significantly higher than that with DTX+LY treatment, particularly at 0.3 μM LY (percent of viable cells: 45.7±1.0% *vs.* 20.5±0.8%, $p<0.001$).

For the three lung cancer cells, the cytotoxicity with DTX→LY and DTX+LY treatment was higher than that with DTX treatment alone and increased with escalation of LY concentration. In particular, a low concentration of DTX→LY effectively inhibited cell proliferation compared with DTX alone or DTX+LY. However, with a high concentration of DTX→LY, cytotoxicity did not increase even with the escalation of LY concentration (Figure 3A).

We calculated the CI values for DTX+LY and DTX→LY treatment for 72 h to compare their effects (Figure 3B). In A549^{G12S} cells, the CIs of DTX+LY and DTX→LY were 0.7 and 0.3 (CI<1; synergism), respectively, and the highest synergistic effect was observed at 0.03 and 0.3 μM LY. In Calu-3^{WT} cells, the CI of DTX→LY (0.03 and 0.3 μM) represented a strong synergistic antitumor activity (CI=0.2 and 0.1, respectively). The CIs of DTX+LY and DTX→LY were less than 0.5, and the greater synergism (CI≤0.2) was observed with DTX→LY treatment. In H727^{G12V} cells, CI could not be calculated as the IC50 was not attained, but the cytotoxicity was similar to that observed in A549^{G12S} cells (Figure 3B).

Synergistic anti-proliferative effect of PTX and LY treatment. We evaluated the synergistic anti-proliferative effect of PTX and LY and compared it with PTX treatment alone in A549^{G12S} and Calu-3^{WT} cell lines.

In A549^{G12S} cells, treatment with a high concentration of PTX followed by treatment with LY strongly inhibited cell proliferation compared to treatment with PTX alone or a low concentration of PTX+LY. In Calu-3^{WT} cells, the cytotoxicity of PTX→LY treatment was markedly higher than that of PTX treatment alone (percent of viable cells: 47.5±0.3% *vs.* 12.7±0.5%, $p<0.001$) (Figure 4A). In A549^{G12S} cells, the CIs

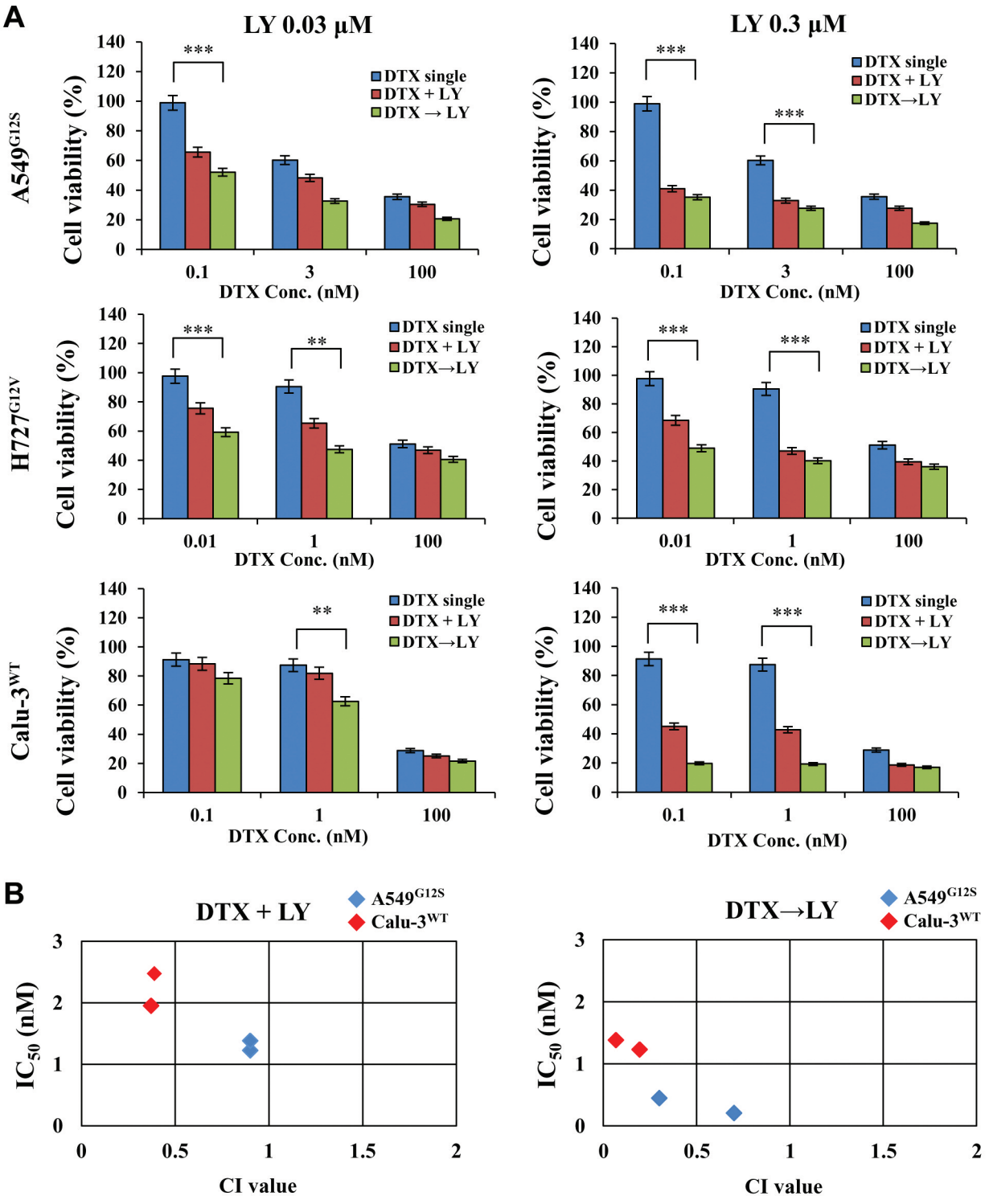

Figure 3. *Anti-proliferative effect of DTX and LY alone and in combination in lung cancer cells. (A) A549^{G12S}, H727^{G12V}, Calu-3^{WT} cells were treated with DTX alone or in combination with LY (0.03 μM and 0.3 μM). Cell viability was quantitatively measured using the CCK-8 assay. (B) Interactions between the DTX and LY drugs were analyzed using combination index (CI). The calculated CIs were divided into 3 categories: CI<1, CI=1, and CI>1, indicating synergistic, additive, and antagonistic effects, respectively. DTX+LY: Simultaneous combination of DTX and LY for 72 h, DTX→LY: sequential treatment with DTX for 24 h followed by LY for 48 h. Each experiment was performed in triplicate. Data represent the mean±SD. *p<0.05, **p<0.01, and ***p<0.001, denote statistically significant differences between the treatment groups and control.*

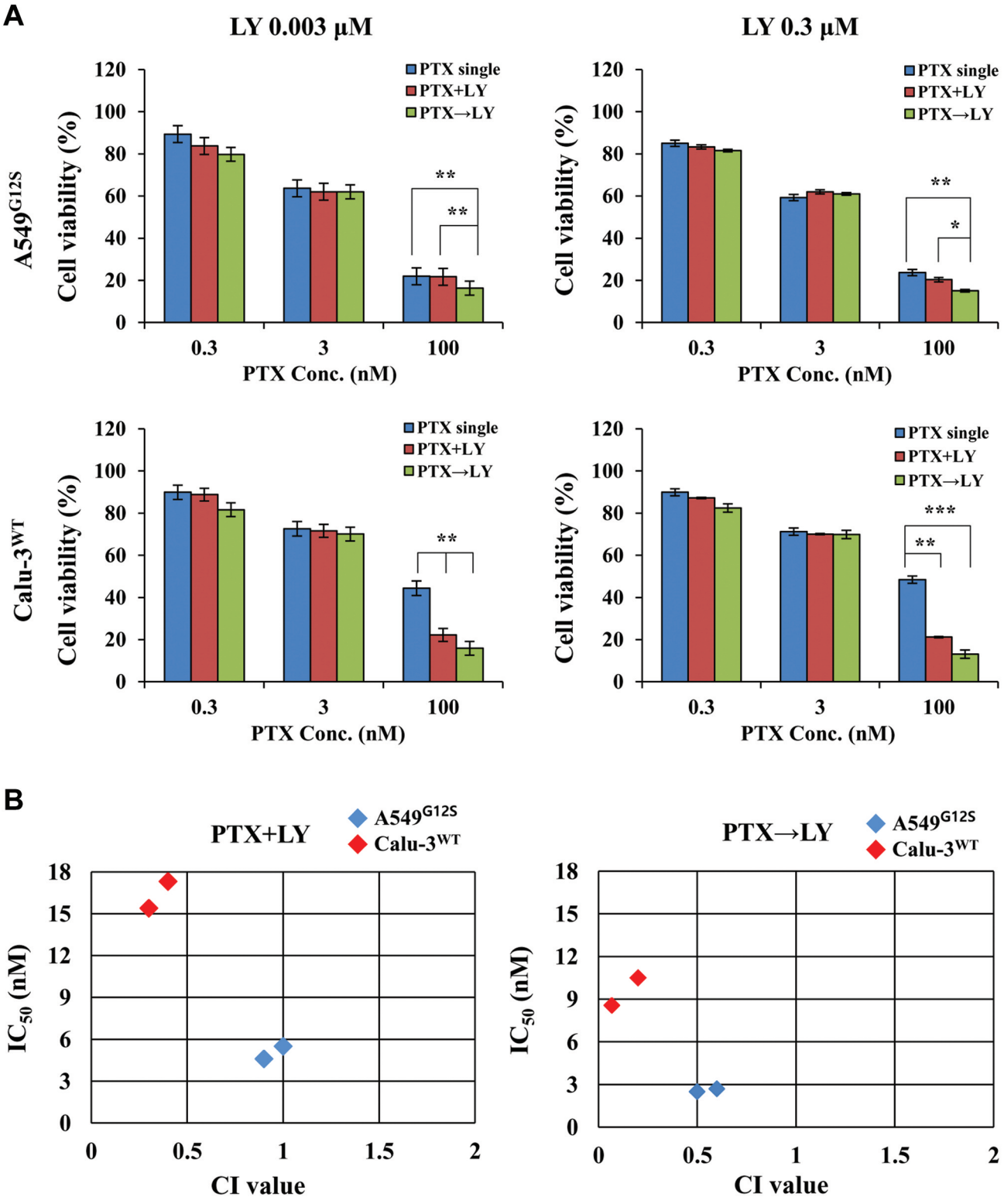

Figure 4. *Anti-proliferative activity of PTX alone and in combination with LY in lung cancer cell lines with or without KRAS mutation. (A) Cells were treated with PTX alone. Cell viability was measured via the CCK-8 assay. (B) Interactions between PTX and LY were analyzed via CI. PTX+LY: simultaneously combined treatment of PTX and LY for 72 h, PTX→LY: sequentially combined treatment with PTX for 24 h followed by LY for 48 h.*

of PTX+LY (0.003 and 0.3 μM) were 0.9 and 1.0, respectively, and those of PTX→LY were 0.5 and 0.6. In Calu-3^{WT} cells, the CIs of PTX+LY (0.003 and 0.3 μM) were 0.3 and 0.4, respectively, and those of PTX→LY were 0.2 and 0.1, respectively (higher synergistic effect) (Figure 4B).

Cell cycle distribution and apoptosis after DTX treatment alone or DTX+LY treatment. We analyzed changes in cell cycle distribution due to treatment with DTX or LY alone, DTX+LY, and DTX→LY (Figure 5A). In DTX→LY, two different concentrations of LY were used according to the cancer cell line (0.003 μM for A549^{G12S} cells and 0.03 μM for H727^{G12V} cells). In A549^{G12S} cells, LY increased G2/M arrested cells by 4.4 times compared with the control (32.6±0.5% *vs*. 7.4±0.1%, $p<0.001$) and LY increased the number of G0/G1 cells by 1.6 times compared with the control (78.7±0.6% *vs*. 48.5±1.0%, $p<0.001$).

For H727^{G12V} cells, LY marginally increased the number of G2/M arrested cells compared with the control (14.2±0.6% *vs*. 12.9±0.5%), with G0/G1 cells (67.0±0.5%) being comparable to the control (63.1±0.6%).

In A549^{G12S} cells, DTX+LY increased the number of G2/M cells by 5.9 times compared with the control (44.2±0.6% *vs*. 7.4±0.1%, $p<0.001$), whereas DTX→LY considerably increased the number of G2/M arrested cells (54.1±0.5% *vs*. 7.4±0.1%, $p<0.001$) and reduced the number of G0/G1 cells (9.2±0.5% *vs*. 83.9±0.3%, $p<0.001$). In H727^{G12V} cells, DTX→LY increased the number of G2/M cells by two times compared with the control (24.4±1.1% *vs*. 12.2±0.6%).

Among A549^{G12S} and H727^{G12V} cells in the DTX group, the proportion of subG1 cells was 7.7±0.2% and 8.7±0.4%, respectively. In A549^{G12S} cells, DTX+LY and DTX→LY increased the number of subG1 cells in a concentration-dependent manner (24.6±1.3% and 26.5±1.2%, respectively). Among H727^{G12V} cells, in the DTX+LY and DTX→LY groups, the proportion of subG1 cells was 9.2±0.3% and 10.8±0.3%, respectively, which was remarkably higher than that in the control (1.2±0.2%).

We measured apoptotic cells to confirm whether cell growth inhibition and increased subG1 (%) contributed to programmed cell death *via* double staining with annexin V-FITC and PI. In A549^{G12S} cells, DTX and LY significantly increased apoptotic cell death by 21.5±4.3% and 25.5±2.2%, respectively, compared with the control (2.6±0.4%). Following simultaneous and sequential administration of DTX (0.1 and 3 nM) and LY (0.003 μM), the proportion of apoptotic cells was 30.1±2.1% and 38.2±4.0% at 0.1 nM of DTX, respectively, and 32.9±3.0% and 42.7±4.5% at 3 nM of DTX, respectively, indicating that DTX→LY significantly increased apoptotic cell death compared with DTX+LY (Figure 5B).

In summary, we found that apoptotic cells increased with higher DTX concentrations and DTX→LY significantly enhanced apoptosis compared with DTX alone or DTX+LY.

Protein expression of KRAS signaling, cell cycle, and apoptosis-related molecules following DTX+LY treatment. We examined the expression of proteins involved in cell cycle regulation, apoptosis, and *KRAS* signaling in A549^{G12S} and H727^{G12V} cells after treatment with DTX and LY alone, DTX+LY, and DTX→LY. DTX and LY diminished the expression of CDK2 and CDK4 in a dose-dependent manner and DTX→LY inhibited the expression more effectively than DTX+LY. DTX→LY also notably inhibited the expression of cyclin B1 compared with DTX and LY alone, or DTX+LY.

DTX and LY alone increased p21 expression in a dose-dependent manner and DTX+LY and DTX→LY significantly increased its expression compared with DTX and LY alone (Figure 6A). DTX alone or in combination treatments increased c-PARP and caspase-3 expression in A549^{G12S} and H727^{G12V} cells. In particular, DTX→LY remarkably upregulated caspase-3 expression in a dose-dependent manner compared with DTX and LY alone or DTX+LY in H727^{G12V} cells (Figure 6B).

We examined *KRAS* expression and its downstream signaling molecules, including p-ERK and MEK, in A549^{G12S} cells. DTX→LY considerably reduced *KRAS* expression compared with DTX and LY alone or DTX+LY. DTX considerably down-regulated p-ERK and MEK expression with increase in concentration. The expression of total ERK is decreased in concentration of DTX alone and LY alone in both A549^{G12S} and H727^{G12V} cells. Pro-PARP and pro-caspase-3 expression was reduced in the DTX and LY alone and in the combination groups in both cells. DTX→LY suppressed the expression of these molecules compared with DTX alone or DTX+LY. LY alone did affect p-ERK expression, but decreased MEK expression in a dose-dependent manner (Figure 6C).

Antitumor effect of PTX+LY in xenograft mice bearing KRAS mutation. We examined the anti-proliferative effect of PTX, LY, and PTX+LY on tumor growth in mouse xenografts bearing A549^{G12S} and H727^{G12V} cells. We determined the treatment schedule based on *in vitro* results showing the potential antitumor effect of combining PTX with LY in six groups including control, PTX20 (PTX alone 20 mg/kg), LY5 (LY alone 5 mg/kg), LY25 (LY alone 25 mg/kg), PTX+LY5 (PTX 20 mg/kg+LY5 mg/kg) and PTX+LY25 (PTX 20 mg/kg+LY 25 mg/kg).

In the case of the A549^{G12S} cell xenograft model, the rate of tumor volume was decreased 32.3% in PTX20, 57.3% and 64.5% in the LY drug concentration (LY5 and LY25) compared to non-drug-treated control group (Figure 7A). In addition, in the case of the PTX+LY combination, the tumor volume was significantly decreased 67.9% in the PTX+LY5 group and 71.8% ($p<0.001$) in the PTX+LY25 group. Furthermore, the tumor volume decreased by 47.6% in LY25 compared to PTX20, and reduced by 33.9% ($p<0.05$) in the

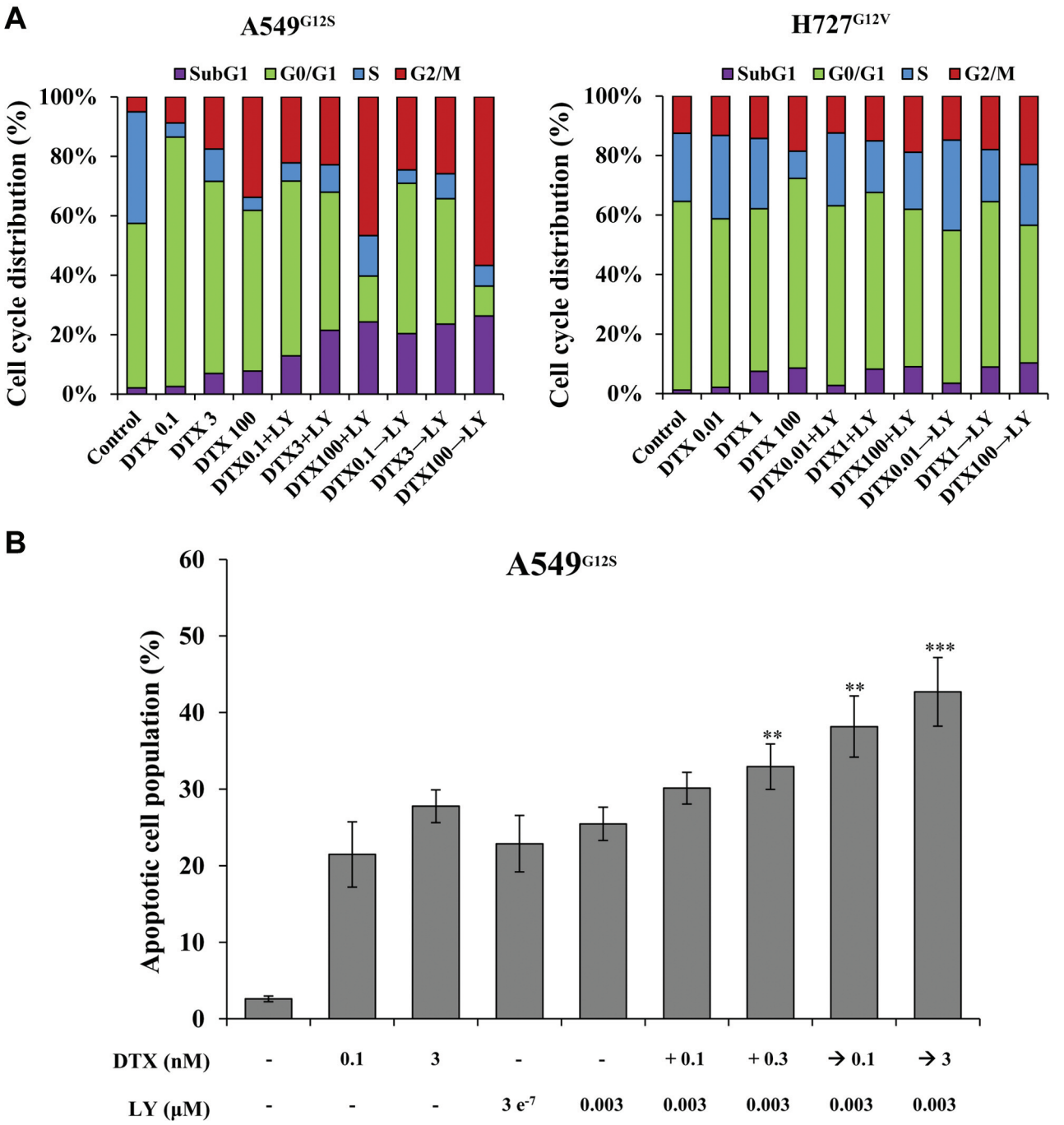

Figure 5. *The changes in cell cycle distribution and apoptosis of cells treated with DTX and LY alone or in combination. A549^{G12S} cells were treated with DTX (0.1, 3, 100 nM) and LY (0.003 μM) simultaneously or sequentially for 72 h. H727^{G12V} cells were treated with DTX (0.01, 1, 100 nM) and LY (0.03 μM) simultaneously or sequentially for 72 h. (A) Cell cycle distribution was analyzed via flow cytometry. (B) Apoptotic population in A549^{G12S} cells, which was analyzed via flow cytometry. Each experiment was performed in triplicate. Data represent the mean±SD. *p<0.05, **p<0.01, and ***p<0.001, denote statistically significant differences between the control and treatment groups.*

PTX+LY 25 group compared to LY5 group. We found that compared to PTX or LY single treatments, the tumor growth inhibition (TGI) values (%) of PTX+LY 25 were 2.2- and 1.1-fold higher than those of PTX20 and LY25 alone (32.3% *vs.* 78.1%, 64.5% *vs.* 78.1%, respectively), and tumor growth delay (TGD) values (%) of PTX+LY 25 were 5.3- and 1.4-

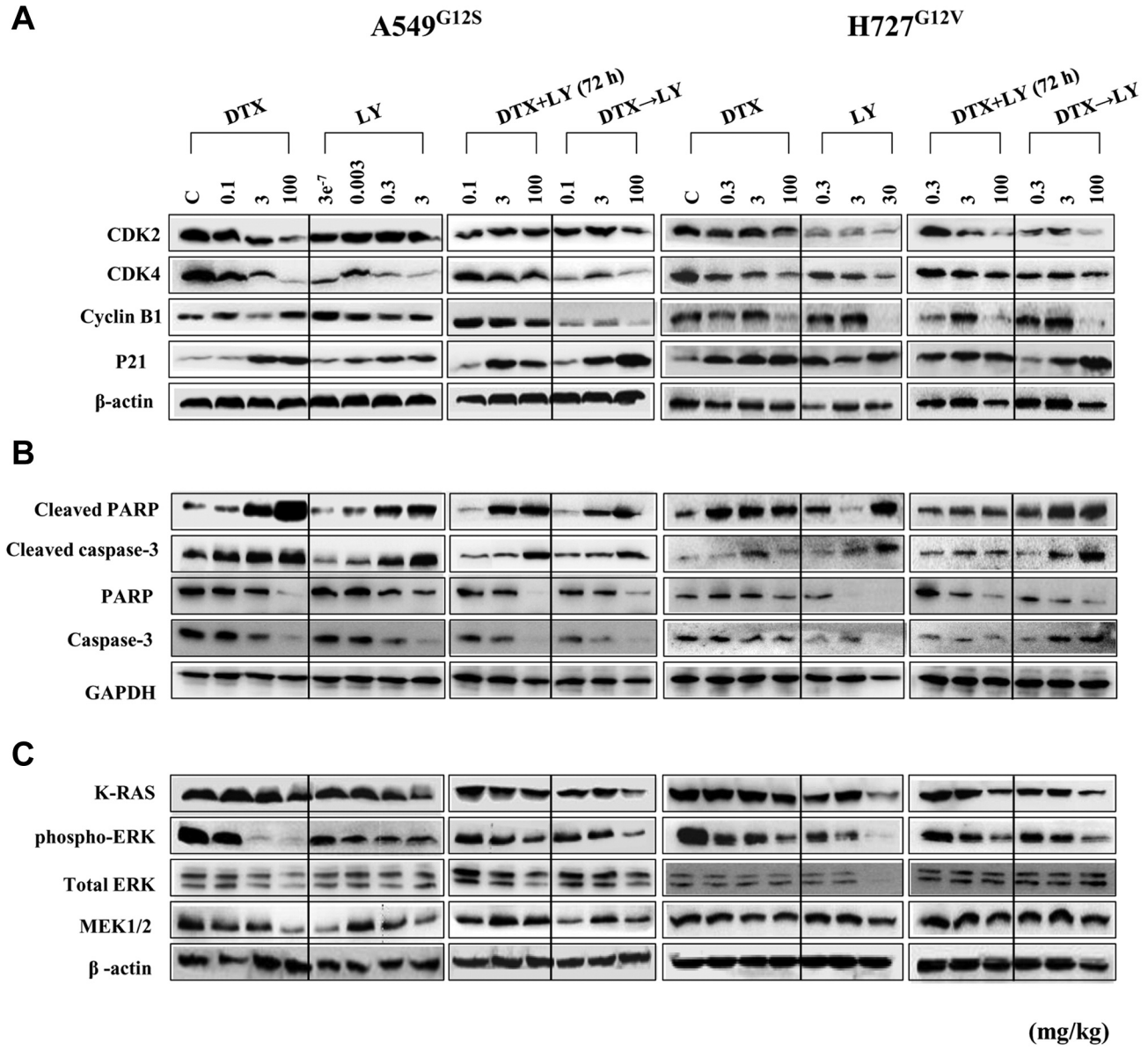

Figure 6. *Expression of proteins involved in cell cycle, apoptosis, and KRAS signaling after treatment with DTX or LY alone, and their combination in A549^{G12S} and H727^{G12V} cells. (A) Expression of cell cycle-related proteins after treatment with DTX or LY alone and their combination. Expression of (B) apoptosis-related proteins and (C) RAS/RAF/ERK signaling proteins. β-actin and GAPDH were used as loading control.*

fold higher than those of the PTX20 and LY25 alone (28.1% *vs*. 149.9%, 107.1% *vs*. 149.9%, respectively) (Table I).

In the H727^{G12V} cell xenograft model, the tumor volume decreased 17.4% in the PTX20 group, 46.5% in the LY5 group, and 51.4% in the LY 25 group compared to the control group (Figure 7B). In addition, the PTX+LY 5 and PTX+LY 25 combinations decreased the tumor size by 54.2% and 68.6% respectively, compared to the control group. In addition, the PTX+LY5 group and the PTX+LY25 group showed significantly decreased tumor volume compared to the control group at 54.2% (1.63±0.27 cm3) and 71.8% (1.12±0.56 cm3, $p<0.001$), respectively. Furthermore, comparing the tumor volume in the PTX20 to PTX+LY 25 groups, PTX+LY25 combined treatment decreased tumor volume to 62.0%. In the H727^{G12V} mouse model, we confirmed that the TGI and TGD values of the PTX+LY25 combination group were 3.9- and 10.4-fold higher than those of PTX20 alone (17.4% *vs*. 68.6%, 6.1% *vs*. 62.7%, respectively). Furthermore, those for PTX+LY25 were 1.3- and 2.1-fold higher than those for LY25 alone

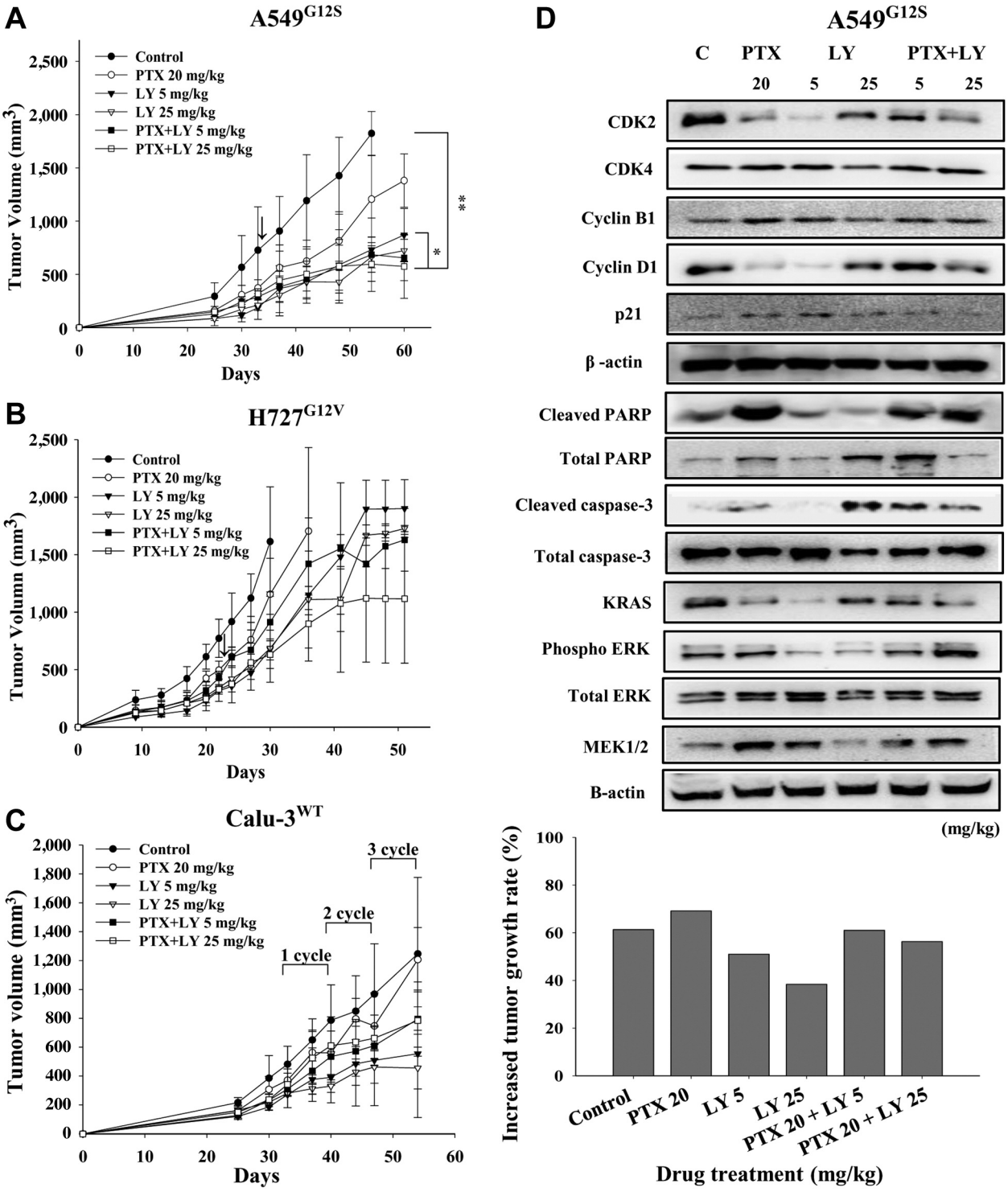

Figure 7. *Enhanced antitumor efficacy of PTX combined with LY in xenograft mice bearing A549^{G12S}, H727^{G12V} and Calu-3^{WT} cells. PTX and LY were administered alone and in combination to assess the capability to retard tumor growth in (A) and (B) xenograft mice bearing A549^{G12S} and H727^{G12V} cells (↓: drug administration start point). (C) The tumor volume and tumor growth rate of PTX and LY treated mice injected with Calu-3^{WT} cells. (D) We evaluated the expression of proteins involved in cell cycle, apoptosis, and KRAS downstream signaling in tumor tissues collected from xenograft mice treated with PTX and LY alone, or their combination. BALB/c nu/nu mice were implanted subcutaneously with 2×10^6 cells. Mice were divided into six groups (control, PTX20 mg/kg, LY5 mg/kg, LY25 mg/kg, PTX+LY5 mg/kg and PTX+LY25 mg/kg; n=5 per group). The values represent the mean±SD for each group. *p<0.01, **p<0.001, denote statistically significant differences.*

Table I. *Tumor growth inhibition and tumor growth delay by LY combined with PTX.*

Groups	PTX	LY	A549^{G12S}		H727^{G12V}	
			% TGI	% TGD (2,000 mm^3)	% TGI	% TGD (2,000 mm^3)
Control	-	-	-	-	-	-
PTX	20 mg/kg	-	32.3	28.1	17.4	6.1
LY	-	5 mg/kg	57.4	79.1	46.5	24.9
	-	25 mg/kg	64.5	107.1	51.4	30.3
PTX+LY	20 mg/kg	5 mg/kg	67.9	124.4	54.2	33.9
	20 mg/kg	25 mg/kg	71.8	149.9	68.6	62.7

PTX: Paclitaxel; LY: LY2835129; TGI: tumor growth inhibition; TGD: tumor growth delay; % TGI: 100-(T/C×100), where T is mean tumor volume of treatment group and C is mean tumor volume of control group; % TGD: (T-C)/C×100, where T is the median time to endpoint of treatment group and C is the median time to endpoint of control group.

(51.4% *vs*. 68.6%, 30.3% *vs*. 62.7%, respectively) (Table I).

In the Calu-3^{WT} cell xenograft model, LY alone (5 mg; 55.5% and 25 mg; 63.4%) was effective in delaying tumor formation, rather than its combination. However, the tumor volume decreased in the PTX+LY combination group compared to the control group (Figure 7C).

To understand the molecular mechanism underlying the antiproliferative activity induced by the combination of PTX and LY, we assessed the expression of proteins involved cell cycle, apoptosis, and *KRAS* signaling in xenograft tumor tissues (Figure 7D). LY decreased CDK2 and KRAS expression, and PTX+LY significantly reduced CDK2 and cyclin D1 expression. However, no significant difference was observed in cyclin B1, total-ERK, and MEK expression between the treatment groups. The expression of p21 increased in LY groups. PTX+LY significantly enhanced c-PARP, total PARP and cleaved caspase-3 expression compared with the control or PTX alone. The phospho-ERK expression reduced in LY alone treatment, but increased in PTX+LY combination group.

Discussion

Significant advances have been made in cancer-targeted treatments in patients with lung adenocarcinomas harboring genetic alterations in driver oncogenes including EGFR, ALK, and ROS1. EGFR-TKIs have become the standard first-line of treatment for advanced NSCLC patients carrying activating EGFR mutations (19-21). *KRAS* mutations are found in 15-20% of NSCLC patients; its prognosis is poor as it confers drug resistance to cytotoxic anticancer drugs (22). Although many preclinical and clinical studies on inhibitors targeting *KRAS* or its downstream signaling molecules have been conducted, more studies are warranted for clinical application (23, 24). Among various combination treatments for overcoming the drug resistance to cytotoxic drugs, taxane-based anticancer drugs combined with the targeted agents such as gefitinib, erlotinib or sunitinib have demonstrated enhanced synergistic antitumor activity (25-28).

LY2835219 (LY), a potent inhibitor of CDK4 and CDK6 controlling G1 cell cycle, effectively suppresses the proliferation of cancer cells (13, 29). In the present study, we observed the synergistic antitumor effect of DTX/PTX combined with LY in lung cancer cells and mouse models regardless of *KRAS* mutations.

A dose-dependent cytotoxicity was observed with DTX or LY treatment alone. Interestingly, LY was highly effective in suppressing cell proliferation regardless of *KRAS* mutations. Higher concentrations of LY reduced tumor cell survival to 10-20% compared with 40% in the DTX treatment group. DTX→LY treatment showed enhanced cytotoxicity compared with DTX treatment alone or DTX+LY treatment. Similarly, PTX→ LY showed greater cytotoxicity than PTX treatment alone or PTX+LY treatment.

A published study reported that LY combined with gemcitabine showed enhanced antitumor activity compared with LY alone in lung cancer cells and xenograft mice harboring *KRAS* mutation (30). Several studies have demonstrated that the sequential treatment with PTX or DTX and EGFR-TKIs was more effective than individual or simultaneous combination treatment of lung cancer cells and mouse models regardless of the EGFR or *KRAS* mutation status (2, 12). The molecular mechanism underlying the antitumor activity of sequential combination therapy has not been elucidated. However, the hypothesis that pre-exposure to EGFR-TKI followed by DTX arrests G1 cell cycle, and cytotoxicity can be reduced by protecting cancer cells from the cytotoxicity of taxanes that arrest G2/M cell cycle is gaining attention (14, 25). We observed that LY→DTX had an additive effect in H727^{G12V} cells, whereas DTX→LY had a synergistic effect, which supports the hypothesis.

By analyzing cell cycle distribution and apoptosis, we confirmed that DTX arrested G2/M cell cycle and LY induced G1 cycle arrest. Comparison of the treatment with DTX alone or in combination with LY indicated that DTX→LY significantly increased the cell fraction in G2/M phase, leading to apoptosis in a DTX concentration-dependent manner. Our data indicated that the potent inhibitory effect on cancer cell proliferation occurred after DTX induced G2/M arrest and LY sequentially arrested cells in the G1 phase. The synergistic cytotoxicity was observed only DTX→LY treatment regardless of *KRAS* mutation. This suggests that the order of administration is an important factor in the synergistic effect.

We examined the expression of proteins involved in the cell cycle, apoptosis, and *KRAS* signaling when the drugs were administered individually or in combination. DTX or LY reduced CDK4 expression and DTX→LY remarkably suppressed CDK4 and cyclin B1 expression. CDK4/cyclin D1 complex plays a critical role in G1/S transition. Cyclin B1 is a subunit that regulates CDK1, which controls progression from G2 to M phase (31-33). They are frequently found to be over-expressed in solid tumors, including breast, head and neck, and NSCLC. Androic *et al*. demonstrated that the down-regulation of cyclin B1 contributed to suppression of cancer cell proliferation and growth induced by PTX treatment in gynecological and breast cancers (34).

With the inhibition of CDKs through a p53-independent mechanism, p21 contributes to apoptosis of arrested cells in the G2/M phase caused by taxanes (16, 35). In the current study, DTX→LY abundantly increased p21 expression and effectively inhibited cell cycle progression. In particular, LY selectively inhibited CDK2 and CDK4 simultaneously and activated p21, thereby inducing the G1 arrest phase, indicating that the inhibition of G1/S transition plays a critical role in DTX→LY-induced enhancement of cytotoxicity. In addition, DTX→LY greatly increased the expression of cleaved PARP and caspase-3 compared with the treatment with individual drugs or their combination. Cleaved PARP and caspase-3, anti-apoptotic proteins, act as critical markers in apoptotic signaling activated by taxanes (36, 37). The increased expression of cleaved PARP is an immediate cell response related to programmed cell death and DNA repair induced by taxanes (38).

We found that treatment with DTX alone or DTX→LY did not have an effect on *KRAS* expression, but significantly diminished p-ERK and MEK1/2 expression. This finding indicates that treatment with DTX alone and DTX→LY effectively suppressed p-ERK and its downstream signaling pathway. Several researchers postulate that the activation of p-ERK signaling pathway plays a critical role in cancer cell proliferation and survival (39) and its inhibition is important for synergetic antitumor effect when EGFR inhibitors are combined with DTX against NSCLC. The synergism of DTX→LY may be attributed to the following mechanisms: 1) apoptosis induced by arresting tumor cells in G2/M phase after DTX treatment; 2) additional apoptosis caused by arresting tumor cells in G1 phase following sequentially treatment with LY, and 3) suppression of activated p-ERK and its downstream signaling molecules by DTX and LY.

In xenograft mice subcutaneously injected with A549^{G12S} and H727^{G12V} cells, we assessed the xenograft tumor growth retardation effect of PTX or LY alone and their combination. We observed that PTX in combination with LY effectively delayed tumor formation compared with PTX or LY alone. In mice injected with Calu-3^{WT}, tumor growth was effectively retarded. PTX combined with LY synergistically inhibited tumor growth in lung cancer xenograft mice regardless of *KRAS* mutation status.

We also examined the expression of proteins involved apoptosis and cell cycle-related in tumor tissues collected from sacrificed mice. CDK2 and CDK4 were increased in the PTX treatment group, and cyclin D1 as well as CDK2 and CDK4 significantly decreased in the PTX+LY treatment group. CDK2 is the major regulator of G1/S cycle progression. Nakayama *et al*. demonstrated that PTX treatment remarkably increased CDK2 expression in breast cancer cells and experimental mice (40), which is in line with our findings. c-PARP and caspase 3 expression was higher in the PTX+LY treatment group than in the PTX treatment group. PTX combined with LY increased CDK2 expression. LY alone reduced the expression of CDK4 involved in the initial step of the G1 phase of the cell cycle and PTX in combination with LY considerably diminished its expression. Gelbert *et al*. reported that the combined treatment with LY and gemcitabine considerably suppressed tumor growth in mice injected with H460 and Calu-6 lung cancer cell lines (30). However, no changes in p-ERK and p-MEK were observed, which are the downstream signaling molecules of *KRAS*.

In the present study, *in vitro* and *in vivo* results demonstrated that DTX treatment alone effectively induced apoptosis with G2/M arrest and significantly suppressed tumor cell proliferation when combined with LY. DTX→LY treatment exhibited greater synergistic antitumor effect than DTX and LY treatment alone or DTX+LY treatment regardless of *KRAS* mutation.

In summary, the sequential treatment with taxane-based anticancer drugs followed by LY2835219, a CDK4/6 inhibitor, is an effective treatment strategy for patients with advanced lung adenocarcinoma with or without *KRAS* mutation.

Conflicts of Interest

None of the Authors have received financial support from the sponsor. The Authors declare no conflicts of interest in association with the present study.

Authors' Contributions

KY Son and MY Kim: Conception and design, analysis, and interpretation of data, writing, review and approval of the manuscript. JO Kim: Analysis of data, review, and approval of manuscript. JY Shin: Analysis of data, review, and approval of manuscript. JH Kang: Conception and design, analysis, and interpretation of data, writing, review and approval of the manuscript. Each Author has read and approved the final version of the manuscript.

Acknowledgements

This research was supported by a grant from the Lilly Pharmaceutical Corporation. We would like to acknowledge the contributions of the Global Nonclinical Research Team at Lilly.

References

1 Zhang C, Zhai S, Li X, Zhang Q, Wu L, Liu Y, Jiang C, Zhou H, Li F, Zhang S, Su G, Zhang B and Yan B: Synergistic action by multi-targeting compounds produces a potent compound combination for human NSCLC both *in vitro* and *in vivo*. Cell Death Dis *5*: e1138, 2014. PMID: 24651441. DOI: 10.1038/cddis.2014.76

2 Zhang XH, Cheng Y, Shin JY, Kim JO, Oh JE and Kang JH: A CDK4/6 inhibitor enhances cytotoxicity of paclitaxel in lung adenocarcinoma cells harboring mutant KRAS as well as wild-type KRAS. Cancer Biol Ther *14(7)*: 597-605, 2013. PMID: 23792647. DOI: 10.4161/cbt.24592

3 Yoon YK, Kim HP, Han SW, Oh DY, Im SA, Bang YJ and Kim TY: KRAS mutant lung cancer cells are differentially responsive to MEK inhibitor due to AKT or STAT3 activation: implication for combinatorial approach. Mol Carcinog *49(4)*: 353-362, 2010. PMID: 20358631. DOI: 10.1002/mc.20607

4 Takezawa K, Okamoto I, Yonesaka K, Hatashita E, Yamada Y, Fukuoka M and Nakagawa K: Sorafenib inhibits non-small cell lung cancer cell growth by targeting B-RAF in KRAS wild-type cells and C-RAF in KRAS mutant cells. Cancer Res *69(16)*: 6515-6521, 2009. PMID: 19638574. DOI: 10.1158/0008-5472.CAN-09-1076

5 Rodriguez-Viciana P, Tetsu O, Oda K, Okada J, Rauen K and McCormick F: Cancer targets in the Ras pathway. Cold Spring Harb Symp Quant Biol *70*: 461-467, 2005. PMID: 16869784. DOI: 10.1101/sqb.2005.70.044

6 Roberts PJ, Bisi JE, Strum JC, Combest AJ, Darr DB, Usary JE, Zamboni WC, Wong KK, Perou CM and Sharpless NE: Multiple roles of cyclin-dependent kinase 4/6 inhibitors in cancer therapy. J Natl Cancer Inst *104(6)*: 476-487, 2012. PMID: 22302033. DOI: 10.1093/jnci/djs002

7 Yuan K, Wang X, Dong H, Min W, Hao H and Yang P: Selective inhibition of CDK4/6: A safe and effective strategy for developing anticancer drugs. Acta Pharm Sin B *11(1)*: 30-54, 2021. PMID: 33532179. DOI: 10.1016/j.apsb.2020.05.001

8 Du Q, Guo X, Wang M, Li Y, Sun X and Li Q: The application and prospect of CDK4/6 inhibitors in malignant solid tumors. J Hematol Oncol *13(1)*: 41, 2020. PMID: 32357912. DOI: 10.1186/s13045-020-00880-8

9 Wang Y, Li X, Liu X, Chen Y, Yang C, Tan C, Wang B, Sun Y, Zhang X, Gao Y, Ding J and Meng L: Simultaneous inhibition of PI3Kα and CDK4/6 synergistically suppresses KRAS-mutated non-small cell lung cancer. Cancer Biol Med *16(1)*: 66-83, 2019. PMID: 31119047. DOI: 10.20892/j.issn.2095-3941.2018.0361

10 Liu M, Liu H and Chen J: Mechanisms of the CDK4/6 inhibitor palbociclib (PD 0332991) and its future application in cancer treatment (Review). Oncol Rep *39(3)*: 901-911, 2018. PMID: 29399694. DOI: 10.3892/or.2018.6221

11 Yu YL, Su KJ, Chen CJ, Wei CW, Lin CJ, Yiang GT, Lin SZ, Harn HJ and Chen YL: Synergistic anti-tumor activity of isochaihulactone and paclitaxel on human lung cancer cells. J Cell Physiol *227(1)*: 213-222, 2012. PMID: 21391217. DOI: 10.1002/jcp.22719

12 Jiang Y, Yuan Q and Fang Q: Schedule-dependent synergistic interaction between docetaxel and gefitinib in NSCLC cell lines regardless of the mutation status of EGFR and KRAS and its molecular mechanisms. J Cancer Res Clin Oncol *140(7)*: 1087-1095, 2014. PMID: 24728492. DOI: 10.1007/s00432-014-1671-x

13 Yadav V, Burke TF, Huber L, Van Horn RD, Zhang Y, Buchanan SG, Chan EM, Starling JJ, Beckmann RP and Peng SB: The CDK4/6 inhibitor LY2835219 overcomes vemurafenib resistance resulting from MAPK reactivation and cyclin D1 upregulation. Mol Cancer Ther *13(10)*: 2253-2263, 2014. PMID: 25122067. DOI: 10.1158/1535-7163.MCT-14-0257

14 Chen B, Zheng J, Zeng Y, Li B, Xie B, Zheng J, Zhou J and Zhang W: Sequence-dependent antiproliferative effects of gefitinib and docetaxel on non-small cell lung cancer (NSCLC) cells and the possible mechanism. PLoS One *9(12)*: e114074, 2014. PMID: 25474307. DOI: 10.1371/journal.pone.0114074

15 Cheng H, An SJ, Zhang XC, Dong S, Zhang YF, Chen ZH, Chen HJ, Guo AL, Lin QX and Wu YL: *In vitro* sequence-dependent synergism between paclitaxel and gefitinib in human lung cancer cell lines. Cancer Chemother Pharmacol *67(3)*: 637-646, 2011. PMID: 20495920. DOI: 10.1007/s00280-010-1347-4

16 Vijayaraghavalu S, Dermawan JK, Cheriyath V and Labhasetwar V: Highly synergistic effect of sequential treatment with epigenetic and anticancer drugs to overcome drug resistance in breast cancer cells is mediated *via* activation of p21 gene expression leading to G2/M cycle arrest. Mol Pharm *10(1)*: 337-352, 2013. PMID: 23215027. DOI: 10.1021/mp3004622

17 Jänne PA, Shaw AT, Pereira JR, Jeannin G, Vansteenkiste J, Barrios C, Franke FA, Grinsted L, Zazulina V, Smith P, Smith I and Crinò L: Selumetinib plus docetaxel for KRAS-mutant advanced non-small-cell lung cancer: a randomised, multicentre, placebo-controlled, phase 2 study. Lancet Oncol *14(1)*: 38-47, 2013. PMID: 23200175. DOI: 10.1016/S1470-2045(12)70489-8

18 Zhang XH, Shin JY, Kim JO, Oh JE, Yoon SA, Jung CK and Kang JH: Synergistic antitumor efficacy of sequentially combined paclitaxel with sorafenib *in vitro* and *in vivo* NSCLC models harboring KRAS or BRAF mutations. Cancer Lett *322(2)*: 213-222, 2012. PMID: 22433711. DOI: 10.1016/j.canlet.2012.03.015

19 La Monica S, Fumarola C, Cretella D, Bonelli M, Minari R, Cavazzoni A, Digiacomo G, Galetti M, Volta F, Mancini M, Petronini PG, Tiseo M and Alfieri R: Efficacy of the CDK4/6 dual inhibitor abemaciclib in EGFR-mutated NSCLC cell lines with different resistance mechanisms to osimertinib. Cancers (Basel) *13(1)*: 6, 2020. PMID: 33374971. DOI: 10.3390/cancers13010006

20 Massarelli E, Varella-Garcia M, Tang X, Xavier AC, Ozburn NC, Liu DD, Bekele BN, Herbst RS and Wistuba II: KRAS mutation is an important predictor of resistance to therapy with epidermal growth factor receptor tyrosine kinase inhibitors in non-small-cell lung cancer. Clin Cancer Res *13(10)*: 2890-2896, 2007. PMID: 17504988. DOI: 10.1158/1078-0432.CCR-06-3043

21 Tanaka T, Matsuoka M, Sutani A, Gemma A, Maemondo M, Inoue A, Okinaga S, Nagashima M, Oizumi S, Uematsu K, Nagai Y, Moriyama G, Miyazawa H, Ikebuchi K, Morita S, Kobayashi K and Hagiwara K: Frequency of and variables associated with the EGFR mutation and its subtypes. Int J Cancer *126(3)*: 651-655, 2010. PMID: 19609951. DOI: 10.1002/ijc.24746

22 Chen H and Zhao J: KRAS oncogene may be another target conquered in non-small cell lung cancer (NSCLC). Thorac Cancer *11(12)*: 3425-3435, 2020. PMID: 33022831. DOI: 10.1111/1759-7714.13538

23 Hamarsheh S, Groß O, Brummer T and Zeiser R: Immune modulatory effects of oncogenic KRAS in cancer. Nat Commun *11(1)*: 5439, 2020. PMID: 33116132. DOI: 10.1038/s41467-020-19288-6

24 Chen K, Zhang Y, Qian L and Wang P: Emerging strategies to target RAS signaling in human cancer therapy. J Hematol Oncol *14(1)*: 116, 2021. PMID: 34301278. DOI: 10.1186/s13045-021-01127-w

25 Pan F, Tian J, Zhang X, Zhang Y and Pan Y: Synergistic interaction between sunitinib and docetaxel is sequence dependent in human non-small lung cancer with EGFR TKIs-resistant mutation. J Cancer Res Clin Oncol *137(9)*: 1397-1408, 2011. PMID: 21796416. DOI: 10.1007/s00432-011-1009-x

26 Furugaki K, Iwai T, Shirane M, Kondoh K, Moriya Y and Mori K: Schedule-dependent antitumor activity of the combination with erlotinib and docetaxel in human non-small cell lung cancer cells with EGFR mutation, KRAS mutation or both wild-type EGFR and KRAS. Oncol Rep *24(5)*: 1141-1146, 2010. PMID: 20878103. DOI: 10.3892/or_00000965

27 Pao W, Wang TY, Riely GJ, Miller VA, Pan Q, Ladanyi M, Zakowski MF, Heelan RT, Kris MG and Varmus HE: KRAS mutations and primary resistance of lung adenocarcinomas to gefitinib or erlotinib. PLoS Med *2(1)*: e17, 2005. PMID: 15696205. DOI: 10.1371/journal.pmed.0020017

28 Shaik MS, Chatterjee A, Jackson T and Singh M: Enhancement of antitumor activity of docetaxel by celecoxib in lung tumors. Int J Cancer *118(2)*: 396-404, 2006. PMID: 16052515. DOI: 10.1002/ijc.21325

29 Ku BM, Yi SY, Koh J, Bae YH, Sun JM, Lee SH, Ahn JS, Park K and Ahn MJ: The CDK4/6 inhibitor LY2835219 has potent activity in combination with mTOR inhibitor in head and neck squamous cell carcinoma. Oncotarget *7(12)*: 14803-14813, 2016. PMID: 26909611. DOI: 10.18632/oncotarget.7543

30 Gelbert LM, Cai S, Lin X, Sanchez-Martinez C, Del Prado M, Lallena MJ, Torres R, Ajamie RT, Wishart GN, Flack RS, Neubauer BL, Young J, Chan EM, Iversen P, Cronier D, Kreklau E and de Dios A: Preclinical characterization of the CDK4/6 inhibitor LY2835219: in-vivo cell cycle-dependent/independent anti-tumor activities alone/in combination with gemcitabine. Invest New Drugs *32(5)*: 825-837, 2014. PMID: 24919854. DOI: 10.1007/s10637-014-0120-7

31 Takahashi T, Yamasaki F, Sudo T, Itamochi H, Adachi S, Tamamori-Adachi M and Ueno NT: Cyclin A-associated kinase activity is needed for paclitaxel sensitivity. Mol Cancer Ther *4(7)*: 1039-1046, 2005. PMID: 16020661. DOI: 10.1158/1535-7163.MCT-04-0282

32 Wang XW, Wang XK, Zhang X, Liang YJ, Shi Z, Chen LM and Fu LW: FG020326 sensitized multidrug resistant cancer cells to docetaxel-mediated apoptosis *via* enhancement of caspases activation. Molecules *17(5)*: 5442-5458, 2012. PMID: 22572929. DOI: 10.3390/molecules17055442

33 Rudolph P, Kühling H, Alm P, Fernö M, Baldetorp B, Olsson H and Parwaresch R: Differential prognostic impact of the cyclins E and B in premenopausal and postmenopausal women with lymph node-negative breast cancer. Int J Cancer *105(5)*: 674-680, 2003. PMID: 12740917. DOI: 10.1002/ijc.11132

34 Androic I, Krämer A, Yan R, Rödel F, Gätje R, Kaufmann M, Strebhardt K and Yuan J: Targeting cyclin B1 inhibits proliferation and sensitizes breast cancer cells to taxol. BMC Cancer *8*: 391, 2008. PMID: 19113992. DOI: 10.1186/1471-2407-8-391

35 Choi YH and Yoo YH: Taxol-induced growth arrest and apoptosis is associated with the upregulation of the Cdk inhibitor, p21WAF1/CIP1, in human breast cancer cells. Oncol Rep *28(6)*: 2163-2169, 2012. PMID: 23023313. DOI: 10.3892/or.2012.2060

36 Bai Z, Ding N, Ge J, Wang Y, Wang L, Wu N, Wei Q, Xu S, Liu X and Zhou G: Esomeprazole overcomes paclitaxel-resistance and enhances anticancer effects of paclitaxel by inducing autophagy in A549/Taxol cells. Cell Biol Int *45(1)*: 177-187, 2021. PMID: 33049093. DOI: 10.1002/cbin.11481

37 Ichite N, Chougule MB, Jackson T, Fulzele SV, Safe S and Singh M: Enhancement of docetaxel anticancer activity by a novel diindolylmethane compound in human non-small cell lung cancer. Clin Cancer Res *15(2)*: 543-552, 2009. PMID: 19147759. DOI: 10.1158/1078-0432.CCR-08-1558

38 Ohtsubo M, Theodoras AM, Schumacher J, Roberts JM and Pagano M: Human cyclin E, a nuclear protein essential for the G1-to-S phase transition. Mol Cell Biol *15(5)*: 2612-2624, 1995. PMID: 7739542. DOI: 10.1128/MCB.15.5.2612

39 Yamamoto T, Ebisuya M, Ashida F, Okamoto K, Yonehara S and Nishida E: Continuous ERK activation downregulates antiproliferative genes throughout G1 phase to allow cell-cycle progression. Curr Biol *16(12)*: 1171-1182, 2006. PMID: 16782007. DOI: 10.1016/j.cub.2006.04.044

40 Nakayama S, Torikoshi Y, Takahashi T, Yoshida T, Sudo T, Matsushima T, Kawasaki Y, Katayama A, Gohda K, Hortobagyi GN, Noguchi S, Sakai T, Ishihara H and Ueno NT: Prediction of paclitaxel sensitivity by CDK1 and CDK2 activity in human breast cancer cells. Breast Cancer Res *11(1)*: R12, 2009. PMID: 19239702. DOI: 10.1186/bcr2231

Received April 28, 2021
Revised August 10, 2021
Accepted August 23, 2021